International Journal of Control, Automation and Systems 16(6) (2018) 2878-2887
http://dx.doi.org/10.1007/s12555-017-0616-y
ISSN:1598-6446 eISSN:2005-4092
http://www.springer.com/12555

Control Algorithms of Magnetic Suspension Systems Based on the Improved Double Exponential Reaching Law of Sliding Mode Control

Jian Pan, Wei Li*, and Haipeng Zhang

Abstract: This paper proposes an improved double power reaching law integral SMC algorithm to overcome the chattering, large overshoot, slow response. This improved algorithm has two advantages. Firstly, the designed control law can reach the approaching equilibrium point quickly when it is away from or close to the sliding surface. The chattering and response speed problems can be resolved. Secondly, the proposed algorithm has a good anti-jamming performance, and can maintain a good dynamic quality under the condition of the uncertain external disturbance. Finally, the proposed algorithm is applied to the open-loop unstable magnetic suspension system. Theoretical analysis and Matlab simulation results show that the improved algorithm has better control performances than the traditional SMC and the power reaching law integral SMC algorithm, such as less chattering, smaller overshoots, and faster response speed.

Keywords: Improved double power reaching law, integral sliding mode control, magnetic suspension systems, Matlab simulation.

1. INTRODUCTION

Some control methods can be applied to many areas [1–4]. Sliding mode control (SMC) has been widely studied for decades because of its simple concept, the strong ability to overcome the interferences and the model uncertainties. It is widely used in industrial systems [5,6]. However, the traditional SMC algorithm has a serious chattering problem, which seriously affects the control accuracy of the system, and even leads to an unstable system [7,8]. Therefore, how to suppress the chattering of the system and improve the dynamic performances of the system has become one of the research hotspots. Some sliding mode control designs assume that the system parameters are known. In this case, we must estimate the parameters of systems by using some identification methods [9–14].

Main methods to solve system chattering problems are the quasi-sliding mode control algorithm [15], the dynamic sliding mode control algorithm [16], the high-order sliding mode control algorithm [17, 18], the LMI-based sliding mode control algorithm [19], the adaptive sliding mode control algorithm [20, 21], the filtering algorithm [22], the disturbance observer algorithm [23], the optimal performance control algorithms [24, 25], the integral sliding mode algorithm [26, 27] and the reaching law algorithm [28–30], etc. The quasi-sliding mode algorithm is a conventional sliding mode control outside the boundary layer. The continuous state feedback control is used in the boundary layer, which effectively weakens the chattering of the system, but reduces the control precision of the system. The disturbance observer algorithm mainly estimates the external interferences and uncertainties, and compensates the interferences, which can suppress the chattering problems caused by the interferences. In some degree, the integral sliding mode control algorithm can effectively deal with the steady-state error caused by certain external disturbances. The typical reaching law algorithms include the constant velocity reaching law, the exponential reaching law and the power reaching law. By adjusting the parameters of the reaching law, not only the dynamic quality of the system arrival process can be guaranteed, but also the high-frequency chattering of the control system can be reduced.

The approaching speed of the constant velocity law algorithm is single and slow, while the exponential law algorithm is fast. However, it is difficult to reach the equilibrium point of the system using the exponential law algorithm when it is close to the sliding surface. When the

Manuscript received October 8, 2017; revised June 14, 2018; accepted July 17, 2018. Recommended by Associate Editor Do Wan Kim under the direction of Editor Won-Jong Kim. This work was supported by the National Natural Science Foundation of China (No. 61602163) and the Science Fund for Distinguished Young Scholars of Hubei Province (No. 2017CFA034). The authors are grateful to Professor Feng Ding at the Jiangnan University (Wuxi, China) for his helpful suggestions.

Jian Pan and Wei Li are with the Hubei Collaborative Innovation Center for High-efficiency Utilization of Solar Energy, Hubei University of Technology, Wuhan 430068, P. R. China (e-mails: jpan12@126.com, wli1235@126.com). Wei Li is also with the Department of Control Science and Engineering, Hubei Normal University, Huangshi 435002, China. Haipeng Zhang is with the China Railway Major Bridge Engineering Group Limited Corporation, Wuhan 430068, P. R. China (e-mail: hpzhang12@126.com).
* Corresponding author.

power reaching law approaches the sliding surface, the velocity of the system is zero, and the equilibrium point of the system can be reached smoothly. However, when the system is away from the sliding surface, the approaching speed of the power reaching law algorithm is slow. However, the novel exponential reaching law still has problems such as chattering problems and slower stabilities. Dadras et al used the method of linear matrix inequality (LMI) to propose a parameter adjustment scheme for the FO integral sliding surface [26]. Wang et al proposed a double power reaching law, which has a good effect in improving the global asymptotic convergence rate and overcomes the problem that the traditional SMC has a large chattering when reaching to the sliding surface [31]. Van et al pointed out that robust non-singular fast terminal sliding mode control has a certain chattering problem [32]. Then, the high-order sliding mode control of the super-twisting algorithm is used to eliminate chattering. However, the above several algorithms are still insufficient in terms of the overshoot of the system and the approaching speed to the sliding surface.

In this paper, we propose an improved double power reaching law integral sliding mode control (DPRL-I-SMC) algorithm. Combined the advantages of the exponential reaching law algorithm and the integral sliding mode control algorithm, the proposed algorithm can approach the sliding surface quickly when the system is away from the sliding surface. When the system is close to the sliding surface, the improved algorithm can reach the equilibrium point of the system smoothly. The results show that the improved DPRL-I-SMC algorithm can effectively eliminate the chattering of the system by using the Lyapunov method. In addition, the approach speed is fast when the system is away from and close to the sliding surface.

2. PROBLEM DESCRIPTION

In this paper, an improved DPRL-I-SMC algorithm is proposed for nonlinear uncertain systems. In order to clarify the basic ideas of the algorithms, firstly, the second-order system is considered. Then the high-order magnetic suspension system is extended.

Consider the following second-order uncertain system,

$$\begin{aligned} \dot{x}_1(t) &= x_2(t) + O^*(t), \\ \dot{x}_2(t) &= a(x,t) + b(x,t)u(t), \\ y(t) &= x_1(t), \end{aligned} \tag{1}$$

where $\boldsymbol{x}(t) = [x_1(t), x_2(t)]^{\mathrm{T}} \in \mathbb{R}^2$ is the system state vector, $u(t) \in \mathbb{R}^2$ is the system control input, $y(t) \in \mathbb{R}^2$ is the system output, $O^*(t)$ represents the uncertain interference of the model of this second-order system, $a(x,t)$ and $b(x,t)$ are polynomials in variable $x(t)$.

Assumption 1: $O^*(t)$ in system (1) is bounded and satisfies $|O^*(t)| \leq D$ where D is a positive number and the upper bound of $O^*(t)$.

2.1. Traditional sliding mode control

Assume that the reference signal is $x_d(t)$. Then the error and its first-order derivative are $e(t) = x_1(t) - x_d(t)$ and $\dot{e}(t) = \dot{x}_1(t) - \dot{x}_d(t)$ respectively, and the second-order derivative is $\ddot{e}(t) = \ddot{x}_1(t) - \ddot{x}_d(t)$. The sliding surface of the traditional sliding mode control is designed as

$$s(t) = re(t) + \dot{e}(t), \tag{2}$$

where r is a constant and satisfies the Hurwitz condition, i.e., $r > 0$. The SMC control law is designed as

$$u(t) = -\frac{1}{b(x,t)}[a(x,t) + r\dot{e}(t) - \ddot{x}_d(t) + \lambda \operatorname{sgn}(s)], \tag{3}$$

where $\lambda \geq 0$ is the gain of the sign function. Define a Lyapunov function $V(t) = [s(t)]^2/2$. From (1) to (3), we have

$$\begin{aligned} \dot{s}(t) &= r\dot{e}(t) + \ddot{e}(t) = r\dot{e}(t) + \ddot{x}_1(t) - \ddot{x}_d(t) \\ &= r\dot{e}(t) + a(x,t) + b(x,t)u(t) + \dot{O}^*(t) - \ddot{x}_d(t). \end{aligned} \tag{4}$$

Combining (1), (3) and (4) gives

$$\begin{aligned} \dot{V}(t) &= s(t)[r\dot{e}(t) + a(x,t) + b(x,t)u(t) + \dot{O}^*(t) - \ddot{x}_d(t)] \\ &= s(t)[-\lambda \operatorname{sgn}(s) + \dot{O}^*(t)] \\ &= -\lambda |s(t)| + s(t)\dot{O}^*(t). \end{aligned} \tag{5}$$

Equation (5) shows that as long as the switching gain in the control law (3) is designed to satisfy $\lambda > D$, the states of system (1) on the sliding surface can reach the sliding surface $s(t) = 0$ in a finite time.

Remark 1: Equation (5) shows that although the control law defined by (3) allows the system to reach the sliding surface in a finite time, the system states still cannot reach the desired balance point position. This is the reason for the existence of the chattering phenomenon in the traditional SMC.

2.2. Power reaching law integral sliding mode control

Many algorithms (such as the traditional SMC algorithm, etc.) cannot eliminate the steady-state errors due to the existence of the interferences or uncertainty factors. However, the integral control is a practical algorithm widely used to eliminate the steady-state error. In order to prove the effectiveness of this algorithm and weaken the chattering problem in the traditional SMC algorithm, and to improve the dynamic performance of the system, it can be analyzed by using the PRL-I-SMC algorithm.

The sliding surface of PRL-I-SMC is defined as

$$s(t) = \dot{e}(t) + r_1 e(t) + r_2 \int_0^t e(\tau) d\tau. \tag{6}$$

The power reaching law is defined as

$$\dot{s}(t) = -\xi |s(t)|^{\delta} \operatorname{sgn}(s). \tag{7}$$

The control law of PRL-I-SMC is designed as

$$\begin{aligned} u(t) = &-\frac{1}{b(x,t)}[a(x,t) + r_1 \dot{e}(t) + r_2 e(t) \\ &- \ddot{x}_d(t) + \xi |s(t)|^{\delta} \operatorname{sgn}(s)]. \end{aligned} \tag{8}$$

where r_1 and r_2 are the constant sliding mode coefficients, ξ is the rate at which the motion point of the system approaches to the switching surface $s(t) = 0$ in the power law, δ is a constant of the power reaching law, and $r_1 > 0$, $r_2 > 0$, $\xi > 0$, $1 > \delta > 0$.

Consider a Lyapunov function $V(t) = [s(t)]^2/2$. Combining (1), (6) and (8) gives

$$\begin{aligned} \dot{s}(t) =& \ddot{e}(t) + r_1 \dot{e}(t) + r_2 e(t) \\ =& \ddot{x}_1(t) - \ddot{x}_d(t) + r_1 \dot{e}(t) + r_2 e(t) \\ =& a(x,t) + b(x,t) u(t) + \dot{O}^*(t) \\ & - \ddot{x}_d(t) + r_1 \dot{e}(t) + r_2 e(t). \end{aligned} \tag{9}$$

Combining (1), (8) and (9) gives

$$\begin{aligned} \dot{V}(t) =& s(t)[a(x,t) + b(x,t)u(t) + \dot{O}^*(t) - \ddot{x}_d(t) \\ & + r_1 \dot{e}(t) + r_2 e(t)] \\ =& s(t)[-\xi |s(t)|^{\delta} \operatorname{sgn}(s) + \dot{O}^*(t)] \\ =& -\xi |s(t)|^{\delta+1} + s(t)\dot{O}^*(t). \end{aligned} \tag{10}$$

Equation (10) shows that as long as the switching gain in the control law (8) is designed to satisfy $\xi > D$, the states of system (1) on the sliding surface can reach the sliding surface $s(t) = 0$ in a finite time.

Remark 2: Equation (10) shows that if the system reaches the sliding surface in a finite time and the disturbance has a continuous steady-state value, then the states may be asymptotically reached the desired equilibrium point position. Although the PRL-I-SMC algorithm can reduce the steady-state error of the system to a certain extent and weaken the chattering of the system, it will make the system produce a certain overshoot problem due to the existence of the integral effect. Thus, an improved DPRL-I-SMC algorithm is proposed.

3. IMPROVED DOUBLE POWER REACHING LAW INTEGRAL SLIDING MODE CONTROL

3.1. Control design

Considering that the existing traditional SMC and PRL-I-SMC algorithms have problems of the slow convergence and the large perturbation, an improved DPRL-I-SMC algorithm is proposed, which can effectively mitigate perturbation problems, reduce the overshoot, and improve the dynamic performance of the PRL-I-SMC algorithm.

According to the PRL-I-SMC algorithm, the sliding surface of DPRL-I-SMC algorithm is designed as

$$s(t) = \dot{e}(t) + r_1 e(t) + r_2 \int_0^t e(\tau) d\tau. \tag{11}$$

The exponential reaching law is designed as

$$\dot{s}(t) = -\lambda_1 \operatorname{sgn}(s) - \xi_1 s(t), \tag{12}$$

where $\lambda_1 > 0$ is the rate at which the motion point of the system approaches to the switching surface $s(t) = 0$ in the exponential reaching law, $\dot{s}(t) = -\xi_1 s(t)$ is the exponential reaching term, $\xi_1 > 0$ is the exponential constant coefficient. The double power reaching law is designed as

$$\dot{s}(t) = -\xi_2 |s(t)|^{\delta_1} \operatorname{sgn}(s) - \xi_3 |s(t)|^{\delta_2} \operatorname{sgn}(s). \tag{13}$$

Although the conventional DPRL algorithm is faster than the PRL algorithm, there are still some chattering issues. The exponential law algorithm can ensure the dynamic quality of the system when it reaches the sliding surface, and it weakens the chattering to some extent. Then an improved DPRL-I-SMC algorithm is proposed. Combining (12) and (13), the reaching law can be designed as

$$\begin{aligned} \dot{s}(t) =& -\lambda_1 \operatorname{sgn}(s) - \xi_1 s(t) - \xi_2 |s(t)|^{\delta_1} \operatorname{sgn}(s) \\ & - \xi_3 |s(t)|^{\delta_2} \operatorname{sgn}(s), \end{aligned} \tag{14}$$

where ξ_2 and ξ_3 are the rates at which the motion points of the system approaches to the switching surface $s(t) = 0$ in the double power law, δ_1 and δ_2 are constants of the power reaching law, and $\xi_2 > 0$, $\xi_3 > 0$, $\delta_1 > 1$, $1 > \delta_2 > 0$.

Lemma 1: The traditional sliding mode control function is $\operatorname{sgn}(s) = \begin{cases} 1, & s > 0 \\ 0, & s = 0, \\ -1, & s < 0 \end{cases}$ Due to the existence of high switching gain, there will be a perturbation phenomenon. However, the use of saturation function $\operatorname{sat}(s) = \begin{cases} \operatorname{sgn}(s), & |s| > \gamma, \\ \frac{s}{\gamma}, & |s| \le \gamma \end{cases}$ can effectively overcome the problem of chattering, where γ is a small positive number.

For system (1), the control law of the proposed improved DPRL-I-SMC algorithm is designed as

$$\begin{aligned} u(t) = &-\frac{1}{b(x,t)}[a(x,t) - \ddot{x}_d(t) \\ & + r_1 \dot{e}(t) + r_2 e(t) + \lambda_1 \operatorname{sat}(s) + \xi_1 s(t) \\ & + \xi_2 |s(t)|^{\delta_1} \operatorname{sat}(s) + \xi_3 |s(t)|^{\delta_2} \operatorname{sat}(s)]. \end{aligned} \tag{15}$$

3.2. Stability analysis

Assumption 2: The perturbations in system (1) are bounded and the system satisfies $\lim_{t\to\infty}\dot{O}^*(t)=0$.

Theorem 1: If the assumption 1 and 2 satisfy system (1), as long as $\dot{O}^*(t)\le\lambda_1$, the system can be asymptotically stable under the condition of the control law (15).

Proof: Taking the derivative of the sliding surface in (11), and combining the system state equation (1) gives

$$\begin{aligned}\dot{s}(t)=&a(x,t)+b(x,t)u(t)+\dot{O}^*(t)-\ddot{x}_d(t)\\&+r_1[\dot{x}_1(t)-\dot{x}_d(t)]+r_2[x_1(t)-x_d(t)].\end{aligned}\tag{16}$$

Substituting (15) into (16) gives

$$\begin{aligned}\dot{s}(t)=&-\lambda_1\mathrm{sat}(s)-\xi_1 s(t)-\xi_2|s(t)|^{\delta_1}\mathrm{sat}(s)\\&-\xi_3|s(t)|^{\delta_2}\mathrm{sat}(s)+\dot{O}^*(t).\end{aligned}\tag{17}$$

Consider a Lyapunov function $V(t)=[s(t)]^2/2$. Taking the derivative of $V(t)$ and combining the above parameters with the constraints give

$$\begin{aligned}\dot{V}(t)=&s(t)\dot{s}(t)\\=&-\lambda_1|s(t)|-\xi_1[s(t)]^2-\xi_2|s(t)|^{\delta_1}|s(t)|\\&-\xi_3|s(t)|^{\delta_2}|s(t)|+\dot{O}^*(t)s(t)\le-[\lambda_1+\xi_1 s(t)\\&+\xi_2|s(t)|^{\delta_1}+\xi_3|s(t)|^{\delta_2}-\dot{O}^*(t)]|s(t)|\\\le&-[\lambda_1-\dot{O}^*(t)]|s(t)|.\end{aligned}\tag{18}$$

From (18), the system states can reach the designed sliding surface $s(t)=0$ of (11) in a finite time to satisfy the stability condition of the system.

4. APPLICATION TO THE MAGNETIC SUSPENSION SYSTEM

4.1. The nonlinear system model

At present, the typical structure of the magnetic suspension system is divided into the conventional suction and the superconducting repulsion type. Germany is the first country to develop TR series of the conventional-type magnetic-type suspension train in 1969. Japan subsequently developed the HSST constant suction medium-low speed magnetic suspension system and introduced the superconducting MLX01 in 1972. China designed the Shanghai magnetic suspension system by introducing the German technology in 2003 and independently developed the Changsha magnetic suspension system in 2015, and they are all conventional suction-type magnetic suspension systems. This type of conventional suction-type magnetic suspension system consists of multiple single-magnet structures. Here, the single magnet structure of conventional suction-type magnetic suspension system is studied. The dynamic model of the single electromagnetic magnetic suspension system can be expressed as

$$m\frac{\mathrm{d}^2\varepsilon(t)}{\mathrm{d}t^2}=mg-F(i,\varepsilon)+f_d(t),\tag{19}$$

$$F(i,\varepsilon)=\frac{\mu_0AN^2}{4}\left(\frac{i(t)}{\varepsilon(t)}\right)^2,\tag{20}$$

$$u(t)=Ri(t)+\frac{\mu_0AN^2}{2\varepsilon(t)}\frac{di(t)}{dt}-\frac{\mu_0AN^2i(t)}{2[\varepsilon(t)]^2}\frac{d\varepsilon(t)}{dt},\tag{21}$$

where m is the mass of the suspension, g is the acceleration of gravity, N is the number of turns of the coil, $F(i,\varepsilon)$ is the electromagnetic attraction, μ_0 is the vacuum permeability, A is the area of the single pole, R is the electromagnet winding resistance, $f_d(t)$ is an external interference, t is time. The system control target is controlled by controlling the voltage $u(t)$ to control the coil current $i(t)$. The ultimate goal is to achieve the output suspension gap $\varepsilon(t)$ of the system to track the desired trajectory.

Let $k'=\frac{\mu_0AN^2}{4}$, and k' be a constant. The state variables $x_1(t)=\varepsilon(t)$, $x_2(t)=\dot{x}_1(t)$ and $x_3(t)=i(t)$ denote the electromagnet suspension gap, velocity and current, respectively. Then the nonlinear state-space model of the magnetic suspension system is depicted by

$$\dot{x}_1(t) = x_2(t),\tag{22}$$

$$\dot{x}_2(t) = g-\frac{k'[x_3(t)]^2}{m[x_1(t)]^2}+\frac{f_d(t)}{m},\tag{23}$$

$$\dot{x}_3(t) = \frac{x_2(t)x_3(t)}{x_1(t)}-\frac{Rx_1(t)x_3(t)}{2k'}+\frac{x_1(t)}{2k'}u(t),\tag{24}$$

$$y(t) = x_1(t),\tag{25}$$

where $y(t)$ is the output suspension gap of the system, $\dot{x}_1(t)$ is the suspension speed of the system, $\dot{x}_2(t)$ is the acceleration of the system, and $\dot{x}_3(t)$ is the derivative of the coil current.

Since the object output $y(t)$ is not related to the control input $u(t)$ directly, the sliding mode controller cannot be directly designed. In order to get the relationship between $y(t)$ and $u(t)$, the system is carried out input and output linearization. Let $O_1(t)=\frac{f_d(t)}{m}$ and take the derivative of $y(t)$. Then the system can be expressed as

$$\dot{y}(t)=\dot{x}_1(t)=x_2(t),\tag{26}$$

$$\ddot{y}(t)=\ddot{x}_1(t)=g-\frac{k'[x_3(t)]^2}{m[x_1(t)]^2}+O_1(t),\tag{27}$$

$$\begin{aligned}y^{(3)}(t)=&x_1^{(3)}(t)\\=&\frac{R[x_3(t)]^2}{mx_1(t)}-\frac{x_3(t)}{mx_1(t)}u(t)+\dot{O}_1(t).\end{aligned}\tag{28}$$

Let $f_1(t)=\frac{R[x_3(t)]^2}{mx_1(t)}$, $g_1(t)=-\frac{x_3(t)}{mx_1(t)}$ and $O(t)=\dot{O}_1(t)$ in order to make the formula easier. Then the system model can be depicted by

$$\begin{cases}x_1^{(3)}(t)=f_1(t)+g_1(t)+O(t),\\y(t)=x_1(t).\end{cases}\tag{29}$$

Assumption 3: In system (29), $O(t)\ge0$, and the limit of disturbance $O(t)$ of this system is $\tilde{O}(t)=\sup_{t>0}|O(t)|$.

4.2. The controller designs and stability analysis

Take the ideal position signal as $x_d(t)$. Then the error and its first-order derivative are $e(t) = x_1(t) - x_d(t)$ and $\dot{e}(t) = \dot{x}_1(t) - \dot{x}_d(t)$, and the second-order derivative is $\ddot{e}(t) = \ddot{x}_1(t) - \ddot{x}_d(t)$. The sliding surface and control law of the traditional sliding mode control are designed as

$$s(t) = c_1 e(t) + c_2 \dot{e}(t) + \ddot{e}(t), \tag{30}$$

$$u(t) = \frac{1}{g_1(t)}\{-f_1(t) + x_d^{(3)}(t) + c_2[\ddot{x}_d(t) - \dot{x}_2(t)] + c_1[\dot{x}_d(t) - x_2(t)] + \eta \operatorname{sgn}(s)\}, \tag{31}$$

where $c_1 > 0$ and $c_2 > 0$ are the sliding mode constant coefficients, $\eta > 0$ is the gain of the sign function.

The sliding surface of PRL-I-SMC is designed as

$$s(t) = c_1 e(t) + c_2 \dot{e}(t) + \ddot{e}(t) + c_3 \int_0^t e(\tau) d\tau. \tag{32}$$

The power reaching law is defined as

$$\dot{s}(t) = -k|s(t)|^{\alpha} \operatorname{sgn}(s). \tag{33}$$

The control law of PRL-I-SMC is designed as

$$u(t) = \frac{1}{g_1(t)}\{-f_1(t) + x_d^{(3)}(t) + c_2[\ddot{x}_d(t) - \dot{x}_2(t)] + c_1[\dot{x}_d(t) - x_2(t)] + c_3[x_d(t) - x_1(t)] + k|s|^{\alpha} \operatorname{sgn}(s)\}, \tag{34}$$

where $c_3 > 0$ is the sliding mode constant coefficient, $k > 0$ is the rate at which the motion point of the system approaches to the switching surface $s(t) = 0$ in the power reaching law, $1 > \alpha > 0$ is the power reaching constant. The sliding surface of DPRL-I-SMC can be designed as

$$s(t) = c_1 e(t) + c_2 \dot{e}(t) + \ddot{e}(t) + c_3 \int_0^t e(\tau) d\tau. \tag{35}$$

The exponential reaching law is designed as

$$\dot{s}(t) = -\eta_1 \operatorname{sgn}(s) - k_1 s(t), \tag{36}$$

where $\eta_1 > 0$ is the rate at which the motion point of the system approaches to the switching surface $s(t) = 0$ in the exponential reaching law, $\dot{s}(t) = -k_1 s(t)$ is the exponential reaching term, $k_1 > 0$ is the exponential constant coefficient.

The double power reaching law is designed as

$$\dot{s}(t) = -k_2|s(t)|^{\alpha_1} \operatorname{sgn}(s) - k_3|s(t)|^{\alpha_2} \operatorname{sgn}(s). \tag{37}$$

Combining (29) and (30), the reaching law of the improved DPRL-I-SMC algorithm is designed as

$$\dot{s}(t) = -\eta_1 \operatorname{sgn}(s) - k_1 s(t) - k_2|s(t)|^{\alpha_1} \operatorname{sgn}(s) - k_3|s(t)|^{\alpha_2} \operatorname{sgn}(s), \tag{38}$$

where $k_2 > 0$ and $k_3 > 0$ are the rates at which the motion point of the system approaches to the switching surface $s(t) = 0$ in the double power law, $\alpha_1 > 1$ and $0 < \alpha_2 < 1$ are power reaching constants.

According to Lemma 1, for system (29), combining (22), (23) and (26), (27) and using the saturation function $\operatorname{sat}(s)$ to replace the symbol function $\operatorname{sgn}(s)$, then the proposed improved DPRL-I-SMC algorithm is designed as

$$u(t) = \frac{1}{g_1(t)}\{-f_1(t) + x_d^{(3)}(t) + c_2[\ddot{x}_d(t) - \dot{x}_2(t)] + c_1[\dot{x}_d(t) - x_2(t)] + c_3[x_d(t) - x_1(t)] + \eta_1 \operatorname{sat}(s) + k_1 s + k_2|s(t)|^{\alpha_1} \operatorname{sat}(s) + k_3|s(t)|^{\alpha_2} \operatorname{sat}(s)\}. \tag{39}$$

In order to verify the effect of the algorithm in the magnetic suspension system, the stability analysis is carried out next.

Assumption 4: The perturbation of system (29) is bounded and satisfies $\lim_{t\to\infty} O(t) = 0$.

Proof: Taking the derivative of the sliding surface (35) and combining (29) and (22), (23) and (26), (27) of the system gives

$$\dot{s}(t) = c_1[\dot{x}_d(t) - x_2(t)] + c_2[\ddot{x}_d(t) - \dot{x}_2(t)] + x_d^{(3)}(t) - f_1(t) - g_1(t)u(t) - O(t) + c_3[x_d(t) - x_1(t)]. \tag{40}$$

Substituting (39) into (40) gives

$$\dot{s}(t) = -\eta_1 \operatorname{sat}(s) - k_1 s(t) - k_2|s(t)|^{\alpha_1} \operatorname{sat}(s) - k_3|s(t)|^{\alpha_2} \operatorname{sat}(s) - O(t). \tag{41}$$

Define a Lyapunov function $V(t) = [s(t)]^2/2$, where $s(t)$ is a sliding surface function with continuous first-order partial derivatives.

Taking the derivative of $V(t)$ and combining with the above parameters of the restrictions gives

$$\begin{aligned} \dot{V}(t) &= -\eta_1|s(t)| - k_1[s(t)]^2 - k_2|s(t)|^{\alpha_1}|s(t)| \\ &\quad - k_3|s(t)|^{\alpha_2}|s(t)| - O(t)s(t) \\ &\le -[\eta_1 + k_1 s(t) + k_2|s(t)|^{\alpha_1} + k_3|s(t)|^{\alpha_2} \\ &\quad + O(t)]|s(t)| \\ &\le 0. \end{aligned} \tag{42}$$

By (42) and the above parameters, the system states can reach the sliding surface $s(t) = 0$ designed in (35) for a limited time. It can be seen that the design satisfies the stable conditions of the system.

5. SIMULATION VERIFICATION

According to the system model (29), in order to evaluate the effectiveness of the proposed algorithm, the

Table 1. The magnetic suspension system parameters.

Symbols	Meanings	Values
m	Suspension quality	750 kg
R	Winding resistance	0.7 Ω
N	Number of turns of the coil	350 turns
A	Single magnet pole area	0.0151 m^2
ε_0	Reference gap	0.01 m
μ_0	Vacuum permeability	$4\pi \times 10^{-7}$ H/m

Table 2. The control parameters of three algorithms.

Algorithms	Parameters
SMC	$c_1 = 144$, $c_2 = 24$, $\eta = 15$
PRL-I-SMC	$c_1 = 144$, $c_2 = 24$, $c_3 = 0.005$ $k = 40$, $\alpha = 0.6$
Improved DPRL-I-SMC	$c_1 = 144$, $c_2 = 24$, $c_3 = 0.005$, $\eta_1 = 15$ $k_1 = 30$, $k_2 = 40$, $k_3 = 4$ $\alpha_1 = 0.7$, $\alpha_2 = 1.1$

proposed improved DPRL-I-SMC algorithm is compared with the traditional SMC and PRL-I-SMC in Matlab. The relevant physical parameters are listed in Table 1.

5.1. Dynamic performance recovery

The initial states of the magnetic suspension system are $x(0) = [0.016,\ 0,\ 0.1]$, the reference input position signal of the system is $\varepsilon_0 = 0.01$m. Simulate and verify the three algorithms of the SMC and the PRL-I-SMC and the improved DPRL-I-SMC algorithms in Matlab. Fig. 1 shows the contrast curves and the partial enlarged graphs of the response of the output gap when the system is stable. Figs. 2–3 are the system input voltage and output current response curves and their partial enlarged graphs. The speed and acceleration curves of the system and their partial enlarged graphs are shown in Figs. 4–5. The control parameters of the three control algorithms are shown in Table 2.

As can be seen from Fig. 1, when the system is suspended near the reference position $\varepsilon_0 = 0.01$m, there is a constant chattering phenomenon and a large overshoot by using the traditional SMC algorithm. In the vicinity of $t = 0.5$s, the gap deviates to 0.06m, the performance recovery time is larger, and there are still chattering problems near the stable point after $t = 1.5$s. Although the PRL-I-SMC algorithm can weaken the chattering, there are some unfavorable factors due to the introduction of the integral control. For example, at $t = 0.2$s, the overshoot of the system using the PRL-I-SMC algorithm is close to 0.03m. In addition, its performance recovery is slower, because the system returns to the stable point until $t = 1.3$s. In contrast to the improved DPRL-I-SMC algorithm, the chattering is substantially eliminated and the overshoot is

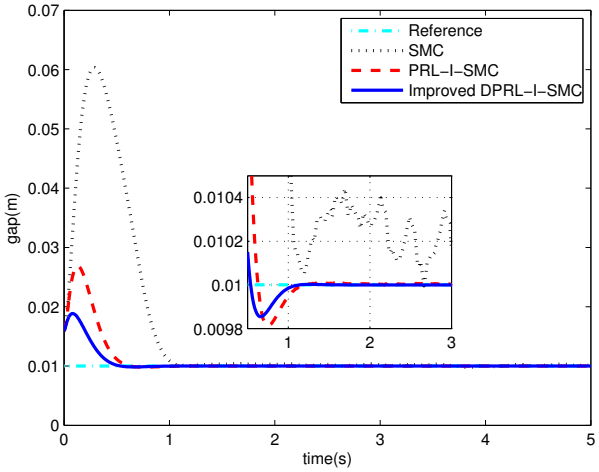

Fig. 1. The responses of the gap.

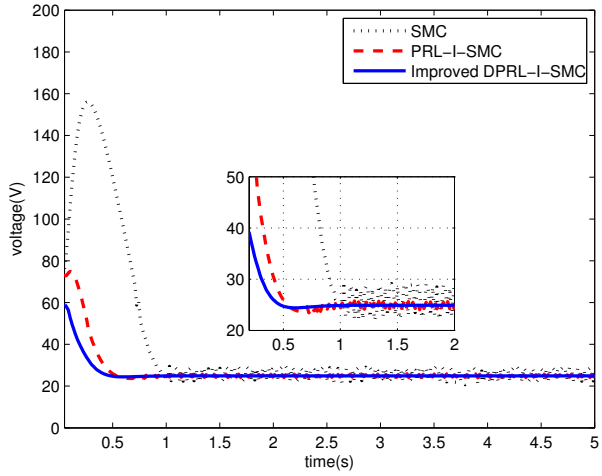

Fig. 2. The responses of the input coil voltage u.

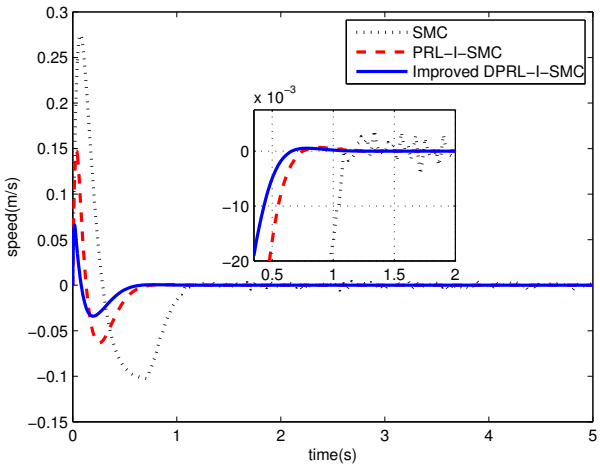

Fig. 3. The responses of the output current i.

reduced. At $t = 0.1$s, the overshoot is only 0.02m, and the performance recovery time is relatively shorter.

It can be seen from Fig. 2 that the maximum input volt-

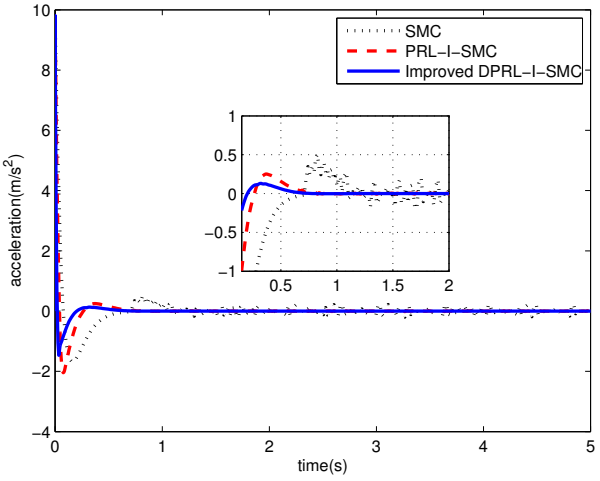

Fig. 4. The responses of the vertical solenoid speed $\dot{x}_1$.

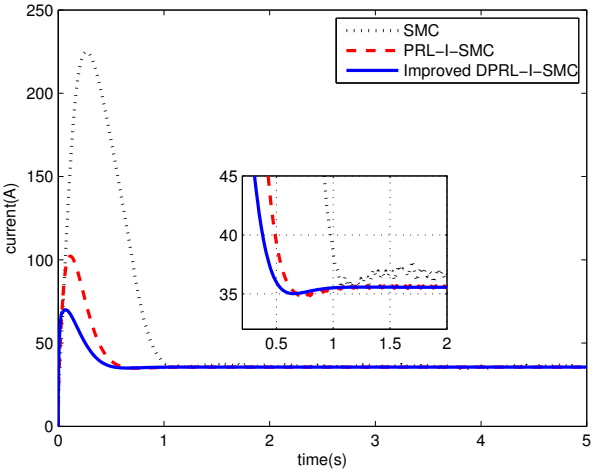

Fig. 5. The responses of the acceleration $\ddot{x}_1$.

age of the improved DPRL-I-SMC algorithm is lower than the maximum input voltage of the conventional SMC and PRL-I-SMC algorithms. There are basically no voltage fluctuations. Fig. 3 shows that the output current of the improved DPRL-I-SMC algorithm is smaller than the output current of the other two algorithms, and there are no current fluctuations.

The output speed and acceleration curves of the system in Figs. 4–5 show that the improved DPRL-I-SMC algorithm is more stable in controlling the system than that of the two other algorithms, and the convergence speed is faster. In summary, the improved DPRL-I-SMC algorithm has better performance in nominal performance recovery than traditional SMC and PRL-I-SMC algorithms.

5.2. The suppression of the sinusoidal interference

The sinusoidal interference force of this perturbation is widespread in practical engineering systems. In this part, the effects of the external disturbances are considered on

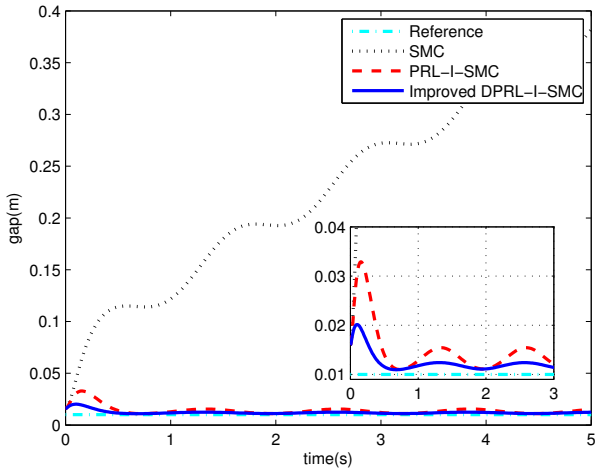

Fig. 6. The response gap for sinusoidal disturbance.

the magnetic suspension control system. Since the external disturbances will reduce the performance of the system, and even lead to instabilities. In order to verify the abilities of the traditional SMC, the PRL-I-SMC control algorithm and the improved DPRL-I-SMC control algorithm to suppress the sinusoidal interference, add the conventional sinusoidal interference signal $d{=}A\sin\omega t+\varphi$ to the system. Consider that the amplitude in the sinusoidal interference force is $A=0.5$, the oscillation period is $\omega=2$, and the displacement is $\varphi=1$. Using the sliding surface and the controller designed in the above three algorithms, the controller parameters are in Table 2.

Fig. 6 is the contrast of the response curves of the gap using the SMC algorithm and the PRL-I-SMC algorithm and the improved DPRL-I-SMC algorithm after adding a sinusoidal interference. Figs. 7 and 8 are the response curves and local magnifications of the input and output currents of the system under the condition of a sinusoidal interference. Figs. 9 and 10 are the comparisons of the speed and acceleration simulation curves and their partial magnifications under a sinusoidal interference condition.

Figs. 6–8 show that the traditional SMC algorithm can cause the gaps and current control to be unstable under the condition of a sinusoidal interference. It can be seen from Fig. 6 that the overshoot and chattering of the improved DPRL-I-SMC algorithm are smaller than those of the PRL-I-SMC algorithm, and the improved DPRL-I-SMC algorithm is faster.

Figs. 7 and 8 show that comparing the improved DPRL-I-SMC algorithm and the PRL-I-SMC algorithm, the maximum input voltage and output current of the former and their fluctuations are smaller.

It can be seen from Figs. 9–10 that compared by the improved DPRL-I-SMC algorithm with the other two algorithms, the vertical solenoid speed and acceleration response curves of the system using the DPRL-I-SMC algorithm are smoother and the reaching speed is faster under

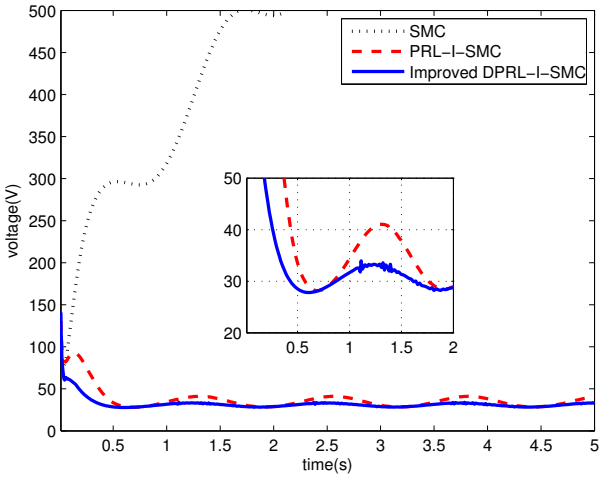

Fig. 7. The response voltage u for sinusoidal disturbance.

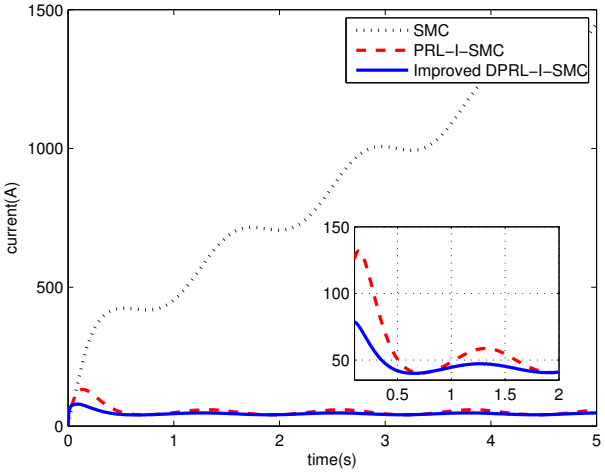

Fig. 8. The response current i for sinusoidal disturbance.

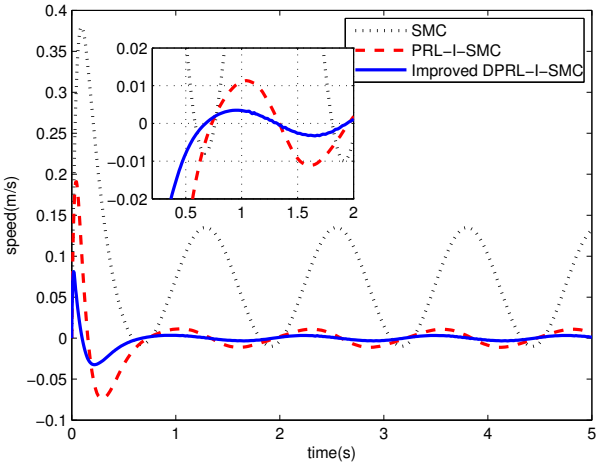

Fig. 9. The response speed $\dot{x}_1$ for sinusoidal disturbance.

the condition of a sinusoidal interference. In conclusion, the improved DPRL-I-SMC algorithm exhibits better anti-jamming performances than the other two algorithms.

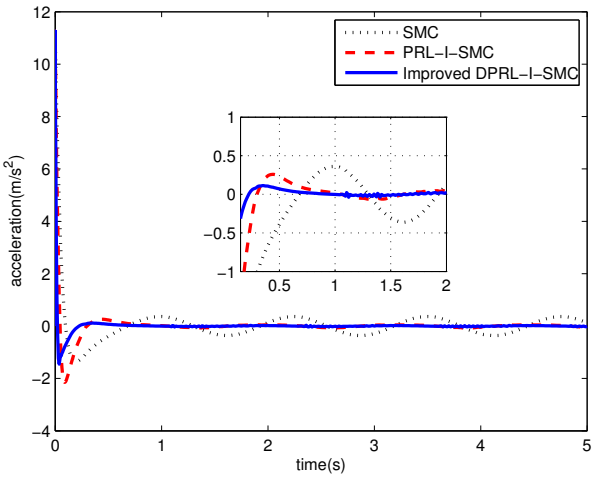

Fig. 10. The response acceleration $\ddot{x}_1$ for sinusoidal disturbance.

6. CONCLUSIONS

This paper proposes an improved DPRL-I-SMC control algorithm, which is applied to the single magnetic structure of magnetic suspension systems. In order to verify the effectiveness of the improved algorithm, the traditional SMC, the PRL-I-SMC and the improved DPRL-I-SMC algorithms are applied to the magnetic levitation system for comparison. The stability of the system is analyzed by Lyapunov function, and the actual nonlinear system model is simulated in Matlab in order to research the anti-jamming performances of the system under a sinusoidal interference. The simulation results show that the improved algorithm can effectively eliminate the chattering of the system, reduce the overshoot, speed up the convergence rate, overcome the nonlinear factors, and make the nonlinear system stable. In short, the improved DPRL-I-SMC algorithm is superior to the traditional SMC and PRL-I-SMC algorithms. The method in the paper can be extended and applied to other fields [33–43] such as the neural network methods [44] and the kernel methods [45, 46].

REFERENCES

[1] Y. Cao, P. Li, and Y. Zhang, "Parallel processing algorithm for railway signal fault diagnosis data based on cloud computing," *Future Generation Computer Systems*, vol. 88, pp. 279-283, November 2018.

[2] Y. Z. Zhang, Y. Cao, Y. H. Wen, L. Liang, and F. Zou, "Optimization of information interaction protocols in cooperative vehicle-infrastructure systems," *Chinese Journal of Electronics*, vol. 27, no. 2, pp. 439-444, March 2018.

[3] Y. Cao, L. C. Ma, S. Xiao, X. Zhang, and W. Xu, "Standard analysis for transfer delay in CTCS-3," *Chinese Journal of Electronics*, vol. 26, no. 5, pp. 1057-1063, September2017.

[4] Y. Cao, Y. Wen, X. Meng, and W. Xu, "Performance evaluation with improved receiver design for asynchronous coordinated multipoint transmissions," *Chinese Journal of Electronics*. vol. 25, no. 2, pp. 372-378, March 2016.

[5] S. L. Shi, K. S. Kang, J. X. Li and Y. M. Fang, "Sliding mode control for continuous casting mold oscillatory system driven by servo motor," *International Journal of Control, Automation and Systems*, vol. 15, no. 4, pp. 1669-1674, August 2017.

[6] S. Islam, P. X. Liu, and A. E. Saddik, "Nonlinear robust adaptive sliding mode control design for miniature unmanned multirotor aerial vehicle," *International Journal of Control, Automation and Systems*, vol. 15, no. 4, pp. 1661-1668, August 2017.

[7] J. L. Chang, "Sliding mode control design for mismatched uncertain systems using output feedback," *International Journal of Control, Automation and Systems*, vol. 14, no. 2, pp. 579-586, April 2016.

[8] C. Pukdeboon, "Output feedback second order sliding mode control for spacecraft attitude and translation motion," *International Journal of Control, Automation and Systems*, vol. 14, no. 2, pp. 411-424, April 2016.

[9] F. Ding, "Decomposition based fast least squares algorithm for output error systems," *Signal Processing*, vol. 93, no. 5, pp. 1235-1242, May 2013.

[10] L. Xu, F. Ding, Y. Gu, A. Alsaedi, and T. Hayat, "A multi-innovation state and parameter estimation algorithm for a state space system with d-step state-delay," *Signal Processing*, vol. 140, pp. 97-103, November 2017.

[11] F. Ding, "Two-stage least squares based iterative estimation algorithm for CARARMA system modeling," *Applied Mathematical Modelling*, vol. 37, no. 7, 4798-4808, April 2013.

[12] Y. J. Liu, D. Q. Wang, and F. Ding, "Least squares based iterative algorithms for identifying Box-Jenkins models with finite measurement data," *Digital Signal Processing*, vol. 20, no. 5, pp. 1458-1467, September 2010.

[13] F. Ding, Y. J. Liu, and B. Bao, "Gradient based and least squares based iterative estimation algorithms for multi-input multi-output systems," *Proceedings of the Institution of Mechanical Engineers, Part I: Journal of Systems and Control Engineering*, vol. 226, no. 1, pp. 43-55, February 2012.

[14] F. Ding, X. P. Liu, and G. Liu, "Gradient based and least-squares based iterative identification methods for OE and OEMA systems," *Digital Signal Processing*, vol. 20, no. 3, pp. 664-677, May 2010.

[15] A. Qureshi and M. A. Abido, "Decentralized discrete-time quasi-sliding mode control of uncertain linear interconnected systems," *International Journal of Control, Automation and Systems*, vol. 12, no. 2, pp. 349-357, April 2014.

[16] S. Mobayen, "An adaptive chattering-free PID sliding mode control based on dynamic sliding manifolds for a class of uncertain nonlinear systems," *Nonlinear Dynamics*, vol. 82, no. 1-2, pp. 53-60, October 2015.

[17] Z. Belkhatir and T. M. Laleg-Kirati, "High-order sliding mode observer for fractional commensurate linear systems with unknown input," *Automatica*, vol. 82, pp. 209-217, August 2017.

[18] J. Yang, J. Y. Su, S. H. Li, and X. H. Yu, "High-Order Mismatched Disturbance Compensation for Motion Control Systems Via a Continuous Dynamic Sliding-Mode Approach," *IEEE Transactions on Industrial Informatics*, vol. 10, no. 1, pp. 604-614, February 2014.

[19] S. Mobayen, D. Baleanu, and F. Tchier, "Second-order fast terminal sliding mode control design based on LMI for a class of non-linear uncertain systems and its application to chaotic systems," *Journal of Vibration and Control*, vol. 23, no. 18, pp. 2912-2925, October 2017.

[20] S. Dadras and H. R. Momeni, "Adaptive sliding mode control of chaotic dynamical systems with application to synchronization," *Mathematics and Computers in Simulation*, vol. 80, no. 12, pp. 2245-2257, August 2010.

[21] H. C. Gui and G. Vukovich, "Adaptive fault-tolerant spacecraft attitude control using a novel integral terminal sliding mode," *International Journal of Robust and Nonlinear Control*, vol. 27, no. 16, pp. 3174-3196, November 2017.

[22] J. Pan, X. Jiang, X. K. Wan, and W. Ding, "A filtering based multi-innovation extended stochastic gradient algorithm for multivariable control systems," *International Journal of Control, Automation and Systems*, vol. 15, no. 3, pp. 1189-1197, June 2017.

[23] D. Ginoya, P. D. Shendge, and S. B. Phadke, "Sliding mode control for mismatched uncertain systems using an extended disturbance observer," *IEEE Transactions on Industrial Electronics*, vol. 61, no. 4, pp. 1983-1992, April 2014.

[24] X. S. Zhan, Z. H. Guan, X. H. Zhang, and F. S. Yuan, "Optimal tracking performance and design of networked control systems with packet dropout," *Journal of the Franklin Institute*, vol. 350, no. 10, pp. 3205-3216, December 2013.

[25] X. S. Zhan, J. Wu, T. Jiang, and X. W. Jiang, "Optimal performance of networked control systems under the packet dropouts and channel noise," *ISA Transactions*, vol. 58, no. 5, pp. 214-221, September 2015.

[26] S. Dadras and H. R. Momeni, "Passivity-based fractional-order integral sliding-mode control design for uncertain fractional-order nonlinear systems," *Mechatronics*, vol. 23, no. 7, pp. 880-887, October 2013.

[27] R. Galván-Guerra, L. Fridman, J. E. Velázquez-Velázquez, S. Kamal, and B. Bandyopadhyay, "Continuous output integral sliding mode control for switched linear systems," *Nonlinear Analysis: Hybrid Systems*, vol. 22, pp. 284-305, November 2016.

[28] S. Chakrabarty and B. Bandyopadhyay, "A generalized reaching law for discrete time sliding mode control," *Automatica*, vol. 52, pp. 83-86, February 2015.

[29] M. H. Rahman, M. Saad, J. P. Kenné, and P. S. Archambault, "Control of an exoskeleton robot arm with sliding mode exponential reaching law," *International Journal of Control, Automation and Systems*, vol. 11, no. 1, pp. 92-104, February 2013.

[30] Y. Q. Chen, Y. H. Wei, H. Zhong, and Y. Wang, "Sliding mode control with a second-order switching law for a class of nonlinear fractional order systems," *Nonlinear Dynamics*, vol. 85, no. 1, pp. 633-643, July 2016.

[31] H. P. Wang, X. K. Zhao, and Y. Tian, "Trajectory Tracking Control of XY Table Using Sliding Mode Adaptive Control Based on Fast Double Power Reaching Law," *Asian Journal of Control*, vol. 18, no. 6, pp. 2263-2271, November 2016.

[32] M. Van, S. S. Ge, and H. L. Ren, "Finite Time Fault Tolerant Control for Robot Manipulators Using Time Delay Estimation and Continuous Nonsingular Fast Terminal Sliding Mode Control," *IEEE Transactions on Cybernetics*, vol. 47, no. 7, pp. 1681-1693, July 2017.

[33] L. Xu, "A proportional differential control method for a time-delay system using the Taylor expansion approximation," *Applied Mathematics and Computation*, vol. 236, pp. 391-399, June 2014.

[34] L. Xu, "Application of the Newton iteration algorithm to the parameter estimation for dynamical systems," *Journal of Computational and Applied Mathematics*, vol. 288, pp. 33-43, November 2014.

[35] L. Xu, L. Chen, and W. L. Xiong, "Parameter estimation and controller design for dynamic systems from the step responses based on the Newton iteration," *Nonlinear Dynamics*, vol. 79, no. 3, pp. 2155-2163, February 2015.

[36] L. Xu, "The damping iterative parameter identification method for dynamical systems based on the sine signal measurement," *Signal Processing*, vol. 120, pp. 660-667, March 2016.

[37] L. Xu, and F. Ding, "Parameter estimation for control systems based on impulse responses," *International Journal of Control, Automation, and Systems*, vol. 15, no. 6, pp. 2471-2479, December 2017.

[38] L. Xu, "The parameter estimation algorithms based on the dynamical response measurement data," *Advances in Mechanical Engineering*, vol. 9, no. 11, pp. 1-12, November 2017.

[39] L. Xu and F. Ding, "Iterative parameter estimation for signal models based on measured data," *Circuits, Systems and Signal Processing*, vol. 37, no. 7, pp. 3046-3069, July 2018.

[40] L. Xu, W. L. Xiong, A. Alsaedi, and T. Hayat, "Hierarchical parameter estimation for the frequency response based on the dynamical window data," *International Journal of Control, Automation and Systems*, vol. 16, no. 4, pp. 1756-1764, August 2018.

[41] F. Ding and H. M. Zhang, "Gradient-based iterative algorithm for a class of the coupled matrix equations related to control systems," *IET Control Theory and Applications*, vol. 8, no. 15, pp. 1588-1595, October 2014.

[42] H. M. Zhang and F. Ding, "Iterative algorithms for X+A(T)X(-1)A=I by using the hierarchical identification principle," *Journal of the Franklin Institute*, vol. 353, no. 5, pp. 1132-1146, March 2016.

[43] H. M. Zhang and F. Ding, "A property of the eigenvalues of the symmetric positive definite matrix and the iterative algorithm for coupled Sylvester matrix equations," *Journal of the Franklin Institute*, vol. 351, no. 1, pp. 340-357, January 2014.

[44] X. Li and D. Q. Zhu, "An improved SOM neural network method to adaptive leader-follower formation control of AUVs," *IEEE Transactions on Industrial Electronics*, vol. 65, no. 10, pp. 8260-8270, October 2018.

[45] F. Z. Geng and S.P. Qian, "An optimal reproducing kernel method for linear nonlocal boundary value problems," *Applied Mathematics Letters*, vol. 77, pp. 49-56, March 2018.

[46] X. Y. Li and B. Y. Wu, "A new reproducing kernel collocation method for nonlocal fractional boundary value problems with non-smooth solutions," *Applied Mathematics Letters*, vol. 86, pp. 194-199, December 2018.

Jian Pan was born in Wuhan, China. He received the B.Sc. degree from the Hubei University of Technology (Wuhan, China) in 1984. He is currently a Professor in the School of Electrical and Electronic Engineering, Hubei University of Technology. His research interests include control science and engineering, computer control and power electronics.

Wei Li was born in Xiaogan, Hubei Province, China. She received the B.Sc. and M.Sc. degrees from the Hubei University of Technology (Wuhan, China), in 2015 and 2018, respectively. She is now an assistant teacher in the Department of Control Science and Engineering, Hubei Normal University, Huangshi, China. Her research interests include system control, multi-agent systems and complex network control.

Haipeng Zhang was born in Wuhan, China. He received the B.Sc. degree in the Mechanical Engineering from the Hubei University of Technology (Wuhan, China) in 2015. He is a mechanical assistant engineer of China Railway Bridge Group Co., Ltd. His research interests include rail transit systems and large machinery control technologies.